

Loss of Thioredoxin Reductase 1 Renders Tumors Highly Susceptible to Pharmacologic Glutathione Deprivation

Pankaj Kumar Mandal¹, Manuela Schneider², Pirkko Kölle³, Peter Kuhlencordt³, Heidi Förster¹, Heike Beck², Georg W. Bornkamm¹, and Marcus Conrad^{1,4}

Abstract

Tumor cells generate substantial amounts of reactive oxygen species (ROS), engendering the need to maintain high levels of antioxidants such as thioredoxin (Trx)- and glutathione (GSH)-dependent enzymes. Exacerbating oxidative stress by specifically inhibiting these types of ROS-scavenging enzymes has emerged as a promising chemotherapeutic strategy to kill tumor cells. However, potential redundancies among the various antioxidant systems may constrain this simple approach. Trx1 and thioredoxin reductase 1 (Txnrd1) are up-regulated in numerous cancers, and Txnrd1 has been reported to be indispensable for tumorigenesis. However, we report here that genetic ablation of Txnrd1 has no apparent effect on tumor cell behavior based on similar proliferative, clonogenic, and tumorigenic potential. This finding reflects widespread redundancies between the Trx- and GSH-dependent systems based on evidence of a bypass to Txnrd1 deficiency by compensatory upregulation of GSH-metabolizing enzymes. Because the survival and growth of Txnrd1-deficient tumors were strictly dependent on a functional GSH system, *Txnrd1*^{-/-} tumors were highly susceptible to experimental GSH depletion *in vitro* and *in vivo*. Thus, our findings establish for the first time that a concomitant inhibition of the two major antioxidant systems is highly effective in killing tumor, highlighting a promising strategy to combat cancer. *Cancer Res*; 70(22); 9505–14. ©2010 AACR.

Introduction

Although the activated oncogene is indispensable for the maintenance of the malignant phenotype (1, 2), reliance on various pathways counteracting the oncogenesis-associated cellular stresses is commonly associated with tumorigenesis, collectively termed as “nononcogene addiction” (3, 4), which could be an Achilles’ heel for cancer. Higher reactive oxygen species (ROS) production, constitutive oxidative stress, and overstrained antioxidant defense systems differentiate tumor cells from their untransformed counterpart (5), as the event

of transformation is followed by increased production of ROS (6–9). This unique feature of tumor cells can be exploited for “selective toxicity” using the redox modifiers like L-buthionine sulfoximine (BSO), ascorbic acid, arsenic trioxide, imexon, phenethyl isothiocyanate, and motexafin gadolinium that selectively kill the tumor cells by perturbing the redox homeostasis (10).

The cellular redox homeostasis is mainly maintained by the thioredoxin (Trx)- and glutathione (GSH)-dependent systems. The Trx system, which consists of Trx, thioredoxin reductase (Txnrd), and Trx-dependent peroxidase (peroxiredoxins), is vital for antioxidant defense, DNA synthesis, and redox-regulated signal transduction, gene expression, and apoptosis (11). Whereas both Trxs and Txnrds are indispensable for embryonic development in mammals (12–16), cytosolic Trx (Trx1) and cytosolic Txnrd (Txnrd1) are essential for cell proliferation (13, 17), as they provide reducing equivalents to ribonucleotide reductase and are thus involved in the maintenance of the deoxynucleotide triphosphate pool (18, 19).

The critical involvement in sustaining high proliferation rates (13, 14, 16) marks the Trx1/Txnrd1 system as a promising drug target for cancer therapy (20). In fact, Trx1 expression level positively correlates with high proliferation capacity, low apoptosis, elevated metastasis (21), increased drug resistance (22), and decreased patient survival (23). By contrast, the role of Txnrd1 in cancer is less clear (24) and could be tumor origin dependent (20). Txnrd1 inactivation by chemical inhibition (25) or small interfering RNA (siRNA)-mediated knockdown (26–28) inhibits self-sufficiency of tumor cells, reverts the malignant phenotype, and sensitizes tumor cells toward

Authors' Affiliations: ¹Institute of Clinical Molecular Biology and Tumor Genetics, Helmholtz Zentrum München, German Research Center for Environmental Health; ²Walter-Brendel Center of Experimental Medicine; and ³Division of Vascular Medicine, Medizinische Poliklinik, Standort Innenstadt, Ludwig-Maximilians-Universität, Munich, Germany; and ⁴German Center for Neurodegenerative Diseases and Helmholtz Zentrum München, Institute of Developmental Genetics, Neuherberg, Germany

Note: Supplementary data for this article are available at Cancer Research Online (<http://cancerres.aacrjournals.org/>).

Current address for P.K. Mandal: Immune Disease Institute, Inc., Harvard Medical School, 200 Longwood Avenue, Boston, MA 02115.

Corresponding Authors: Pankaj Kumar Mandal and Marcus Conrad, German Center for Neurodegenerative Diseases and Helmholtz Zentrum München, Institute of Developmental Genetics, Ingolstädter Landstrasse 1, 85764 Neuherberg, Germany. Phone: 498931874608; Fax: 498931873099; E-mail: pankaj.mandal@helmholtz-muenchen.de, marcus.conrad@helmholtz-muenchen.de.

doi: 10.1158/0008-5472.CAN-10-1509

©2010 American Association for Cancer Research.

the oxidative stress-inducing agents H₂O₂ and ionizing radiation (29). However, the lack of genetic models had thus far precluded to unequivocally assign a crucial role to Txnrd1 in tumorigenesis because of the intertwined functions of Trx1 and Txnrd1. Moreover, the degree of redundancies among various antioxidant systems in cancer has remained obscure. Using a genetic approach, we show that targeted disruption of *Txnrd1* has hardly any effect on proliferation and clonogenic or tumorigenic potential of transformed cells. Furthermore, we identify distinct alterations in GSH metabolism, which compensate for the lack of Txnrd1, rendering knockout tumor cells highly susceptible to GSH deprivation.

Materials and Methods

Materials

Unless stated otherwise, all chemicals were purchased from Sigma-Aldrich. pBJ3 Ω *c-myc* and pUC EJ6.6 *H-ras*^{v12} were kindly provided by Dr. Hartmut Land. For gene transfer, the lentivirus vector system was used as described (30). Antibodies against human Trx and Txnrd1 were kindly provided by Dr. Vadim Gladyshev (Redox Biology Center). The Tat-Cre protein was a generous gift from Dr. W. Hammerschmidt (Helmholtz Zentrum München). Antibodies against glutathione *S*-transferases (GST), heme oxygenase-1 (HMOX1), and aldehyde oxidase 1 (AOX1) were kindly provided by Dr. Dolph Hatfield (NIH).

Isolation of mouse embryonic fibroblasts, establishment of transformed *Txnrd1*^{-/-} cell lines, and reconstitution of Txnrd1 expression

Mouse embryonic fibroblasts (MEF), isolated from conditional *Txnrd1* knockout mouse embryos (13), were transformed by cotransducing them with *c-myc*- and *H-ras*^{v12}-expressing lentiviruses. *In vitro* deletion of *Txnrd1* was achieved by treating the cells with Tat-Cre fusion protein (31). For reconstitution, the *Txnrd1*^{-/-} cells were stably transfected with the tetracycline-inducible expression vector pRTS-1-SF-Txnrd1 (32). For induction, doxycycline (Dox), a semisynthetic tetracycline that is active at lower concentration and more stable than tetracycline, was used throughout this study.

MTT assay

Cell proliferation and cytotoxicity were measured by the MTT assay as described (ref. 33; Supplementary Data).

Western blot

SDS-PAGE and Western blotting were performed as described previously (30).

Cell cycle analysis

The cell cycle analysis was done by the propidium iodide (PI) method (34), and data were analyzed by ModFitLT V3.0 software (Supplementary Data).

Soft agarose assay

Five hundred cells per well were plated in 0.3% soft agarose prepared in cell culture medium in a six-well cell culture

plate and allowed to grow for 10 days. Colonies were fixed in methanol, stained with 0.5% crystal violet, and counted.

Quantitative reverse transcription-PCR

Quantitative reverse transcription-PCR (RT-PCR) was carried out by using the LightCycler FastStart DNA MasterPLUS SYBR Green I kit in combination with the LightCycler 1.5 System (Roche Diagnostic). Expression was normalized against *18S* RNA and presented as fold change with respect to the parental cells.

Measurement of GSH concentration by high-performance liquid chromatography

GSH concentrations were measured by the isocratic high-performance liquid chromatography as described (35).

Determination of GSH reductase activity

GSH reductase (GR) activity was measured by monitoring the decrease in absorbance at 340 nm wavelength resulting from consumption of NADPH (36) in a 96-well plate (Supplementary Data).

Generation of Txnrd1-deficient B-cell lymphoma mice

To achieve B cell-specific deletion of *Txnrd1*, conditional *Txnrd1* knockout mice (*Txnrd1*^{f/f}; ref. 13) were bred with B cell-specific Cre-expressing mice (*mb-1* Cre; ref. 37). To address the role of Txnrd1 in *c-myc*-driven B-cell lymphoma, *Txnrd1*^{f/f};*mb-1* Cre mice were crossed with λ -*myc* mice (38). The breeding scheme is shown in Fig. 3A.

Subcutaneous implantation of transformed cells into C57BL/6 mice

For s.c. tumor transplantation experiments, 8-week-old C57BL/6 mice were purchased from Janvier. Transformed cells (1×10^5) in a final volume of 100 μ L were injected s.c. into the mice. After 12 days of tumor growth, mice were sacrificed, and the tumor mass was determined. Mice were kept under standard conditions with food and water ad libitum (Ssniff). All animal experiments were performed in compliance with the German animal welfare law and have been approved by the institutional committee on animal experimentation and the government of Oberbayern.

Treatment of Txnrd1^{-/-} tumor-bearing mice with BSO

Transformed *Txnrd1*^{-/-} cells (1×10^5) and the parental *Txnrd1*^{f/f} cells were implanted s.c. into C57BL/6 mice. Tumors were allowed to settle for 3 days. Then, BSO (20 mmol/L) was provided in drinking water for 10 days. BSO-containing water was changed twice a week. At the end of the experiment, mice were sacrificed, and the tumor mass was determined.

Results

Transformation and *in vitro* deletion of Txnrd1 in conditional Txnrd1 knockout MEFs

To address the supposedly vital role of Txnrd1 in oncogenesis by genetic means, we generated immortalized MEF cell

lines from conditional *Txnrd1* knockout mouse embryos (two *Txnrd1^{fl/fl}* and one *Txnrd1^{+/-}*; fl, floxed). This became necessary as we had invariably failed to establish MEFs directly from *Txnrd1^{-/-}* embryos (13). The gene targeting strategy previously used for targeted disruption of *Txnrd1* is depicted in Fig. 1A (13). We used *Txnrd1^{fl/fl}* and *Txnrd1^{+/-}* cells as parental cell lines to exclude potential clonal effects during isolation and subsequent culturing. Moreover, the floxed *Txnrd1* allele was shown to behave like wild-type *Txnrd1* allele (13). Therefore, we considered the

Txnrd1^{fl/fl} and *Txnrd1^{+/-}* cells as best available controls for the following experiments. The procedure of establishing transformed *Txnrd1^{-/-}* cell lines is schematically depicted in Fig. 1B. Transformation of the immortalized fibroblasts was achieved by the well-established cooperative action of the two oncogenes *c-myc* and *H-ras^{V12}* (39). Outgrowing single-cell colonies in soft agar were individually picked and expanded to establish the clonally transformed cell lines. Expression of *c-myc* and *H-ras^{V12}* in these clones was confirmed by immunoblotting (Fig. 1C). Transformed

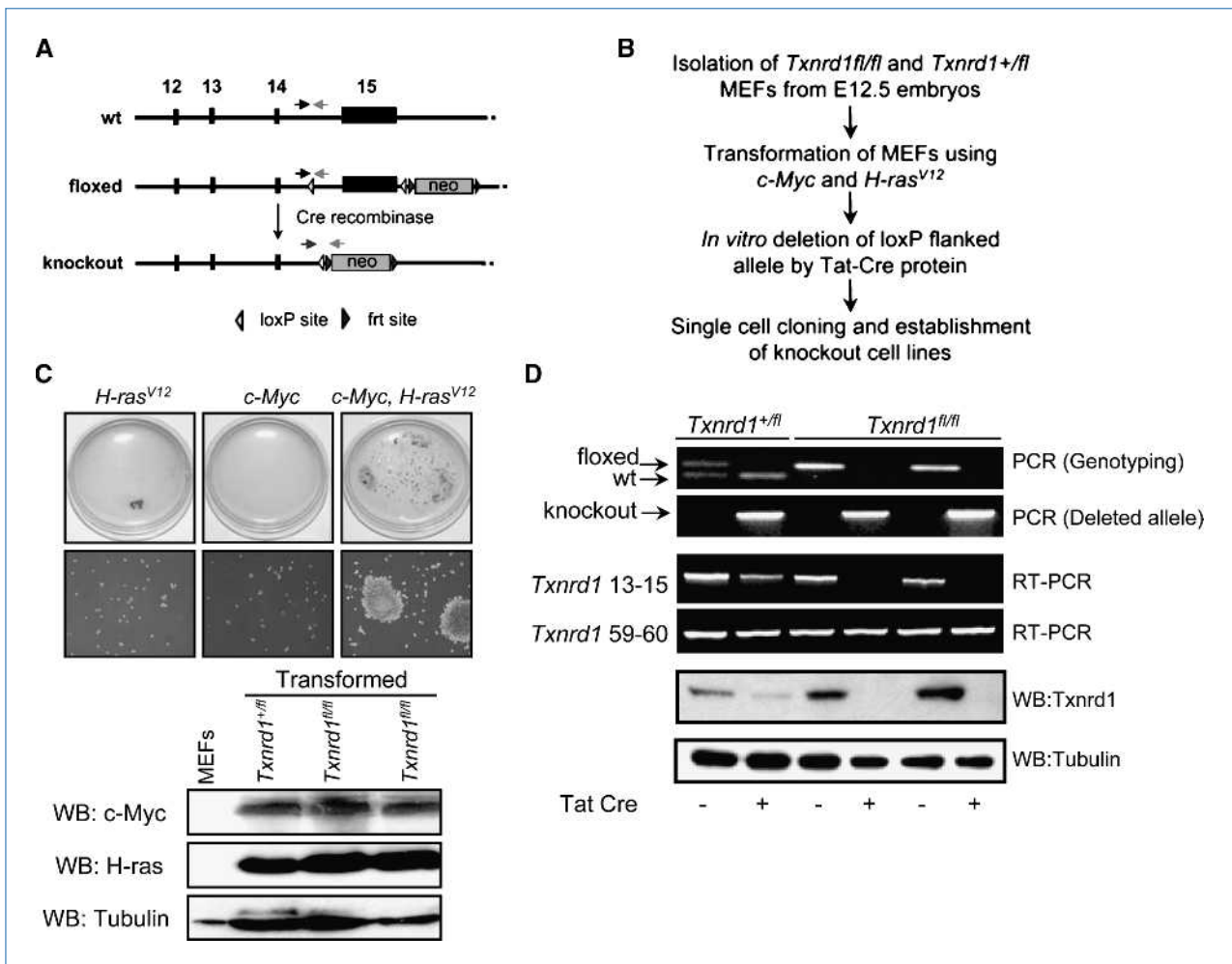


Figure 1. Disruption of *Txnrd1* in MEFs by Cre *ex vivo*. **A**, schematic representation of the generation of conditional *Txnrd1* knockout mice (13). Exon 15 of *Txnrd1*, harboring the COOH terminal catalytic center, was flanked by loxP sites (white triangles), which can be targeted by Cre recombinase. Primer pairs used for genotyping of mice and cells are depicted as black and gray arrows. **B**, experimental outline of how transformed *Txnrd1^{-/-}* cell lines were established. **C**, *in vitro* transformation of MEFs. MEFs were transduced with *c-myc*- and *H-ras^{V12}*-expressing lentiviruses. The event of transformation was only noticed when cells were cotransduced with *c-myc* and *H-ras^{V12}* lentiviruses in the form of outgrowing colonies in soft agar. Single-cell clones were picked and expanded to establish clonal cell lines. Overexpression of *c-Myc* and *H-ras^{V12}* was confirmed by immunoblotting (bottom). **D**, genotype of transformed MEF cell lines. Transformed MEF cell lines were treated with Tat-Cre protein. Successful deletion of the gene was verified by PCR using the deletion-specific primer pairs (as depicted in **A**). The 66-bp band corresponds to the wild-type allele, the 130-bp band corresponds to the floxed allele, and the 320-bp band is obtained after successful deletion of the loxP-flanked allele. Deletion in these cell lines was further confirmed by semiquantitative RT-PCR. RT-PCR amplification using primer pair *Txnrd1* 13-15 yielded no product, confirming the deletion of *Txnrd1* at the mRNA level. The upstream primer pair *Txnrd1* 59-60 generated products in all cases, which indicated the production of truncated mRNA transcripts confirming our previous report (13). Western blot results using a *Txnrd1*-specific antibody showed that no truncated *Txnrd1* protein was generated.

Txnrd1^{-/-} cell lines were established by treatment of the transformed cells with Tat-Cre protein followed by single-cell cloning (see Supplementary Data for detailed procedure). Knockout of *Txnrd1* in the resulting clones was confirmed by PCR, RT-PCR, and immunoblotting (Fig. 1D). Transformed *Txnrd1*^{fl/fl} parental cells and knockout cells derived from them are called *Txnrd1*^{fl/fl} and *Txnrd1*^{-/-} in the following, respectively.

***Txnrd1* deficiency does not impair the proliferation of transformed MEFs**

Several previous reports, including our unsuccessful attempts to establish *Txnrd1*^{-/-} cell lines directly from knockout embryos (13), indicated an indispensable role for *Txnrd1* in proliferation (13, 17) and tumorigenesis (25–28). Yet, by the procedure described above, we succeeded in generating *Txnrd1*^{-/-} cell lines. A comparative analysis revealed that there was no difference in the proliferation rate of *Txnrd1*^{fl/fl} and *Txnrd1*^{-/-} cells (Fig. 2A). Because the cytosolic Trx system has been implicated in cell proliferation, for example, by providing reducing equivalents to ribonucleotide reductase (18, 19), we hypothesized that cell cycle phases might be altered in *Txnrd1*^{-/-} cells. But there was no alteration in cell cycle distribution of *Txnrd1*^{-/-} cells (G₀-G₁, 33.85 ± 4.7%; S, 52.33 ± 0.8%; G₂-M, 13.81 ± 3.8%) compared with the *Txnrd1*^{fl/fl} cells (G₀-G₁, 34.55 ± 1.1%; S, 48.76 ± 2.3%; G₂-M, 16.68 ± 3.5%; Fig. 2B). This is in line with earlier reports that knockdown of *Txnrd1* has no effect on cell cycle progression under normal culture conditions (27), whereas under serum-deprived conditions, transition through S phase is delayed (28).

siRNA-mediated knockdown (26–28) or chemical inhibition (25) of *Txnrd1* has been reported to cause the reversal of malignant phenotype and loss of clonogenicity and tumorigenicity. At variance to this expectation, *Txnrd1*^{-/-} cells were able to form colonies in soft agar to the same extent as *Txnrd1*^{fl/fl} cells (153 ± 21 versus 215 ± 9; Fig. 2C). Moreover, *Txnrd1*^{-/-} cells formed tumors of comparable mass (0.57 ± 0.18 g) on s.c. implantation into C57BL/6 mice like the *Txnrd1*^{fl/fl} cells (0.59 ± 0.25 g; Fig. 2D). Similar results were obtained with another pair of cell lines (data not shown). This indicated that the loss of *Txnrd1* had no effect on clonogenicity and tumorigenicity of transformed cells.

***Txnrd1* is dispensable for *c-myc*-driven B-cell lymphomagenesis**

Previously, we found that *Txnrd1* is a target gene of the oncogene *c-myc* (40). To address the role of *Txnrd1* in B-cell lymphomagenesis, we crossed the conditional *Txnrd1* knockout mice (13) with λ -*myc* mice (38), which develop lymphoma of immature B-cell origin. B cell-specific deletion of *Txnrd1* was achieved by crossing *Txnrd1*^{fl/fl} mice with B cell-specific Cre-expressing mice (*mb-1* Cre mouse; ref. 37). The *mb-1*-driven Cre is expressed at the very early pro-B-cell stage and is therefore the best available pan-B cell-specific Cre mouse strain. The breeding strategy and genotyping of the mice are depicted in Fig. 3A. To our surprise, there was no effect of *Txnrd1* deletion on lymphoma development and

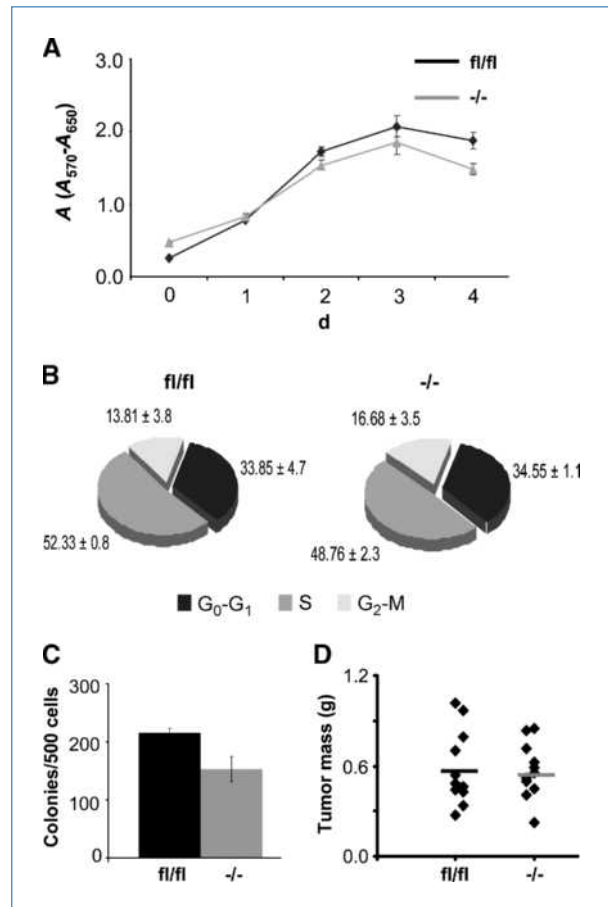


Figure 2. Loss of *Txnrd1* has no effect on proliferation, cell cycle progression, clonogenicity, and tumorigenicity of transformed cells. A, *Txnrd1*^{-/-} cells showed equal proliferation propensity as *Txnrd1*^{fl/fl} cells measured by MTT assay. Data are representative of two independent experiments performed in quadruplicates. B, PI staining of asynchronously growing *Txnrd1*^{-/-} cells showed comparable cell cycle distribution profile as *Txnrd1*^{fl/fl} cells. The pie diagram represents the pooled data from two independent experiments (mean ± SD in %). C, similar numbers of colonies were formed by *Txnrd1*^{-/-} cells (153 ± 21) and *Txnrd1*^{fl/fl} cells (215 ± 9) per 500 cells seeded in soft agar. The experiment was done in triplicate and is representative of two independent experiments. D, s.c. transplantation of 1×10^5 transformed *Txnrd1*^{-/-} and *Txnrd1*^{fl/fl} cells into the flanks of C57BL/6 mice gave rise to tumors of comparable masses (0.57 ± 0.18 versus 0.59 ± 0.25, respectively; mean ± SD) after 12 d of tumor growth ($n = 11$; total number of tumor analyzed).

survival in diseased mice as shown in Fig. 3B. Ten of 11 *Txnrd1*^{fl/fl};Cre⁺;myc⁺ mice developed tumors (median survival period of 117 ± 39.4 days) with comparable incidence with *Txnrd1*^{fl/fl};Cre⁺;myc⁺ mice (9 of 11 succumbed to the disease with a median survival of 108 ± 69.7 days; Fig. 3B). *Txnrd1* knockout was confirmed by semiquantitative RT-PCR using primer pairs binding in exons 13 and 15 of murine *Txnrd1* (Fig. 3C). Having shown that loss of *Txnrd1* has no effect on tumor growth in two different tumor models, fibrosarcoma and *myc*-driven B-cell lymphoma, we hypothesized a compensatory upregulation of a yet unrecognized pathway as a plausible explanation.

Upregulation of GSH metabolizing enzymes is observed under Txnrd1 deficiency

To study the compensatory mechanisms rendering Txnrd1 dispensable for cell proliferation and tumor development, we used the Txnrd1-deficient transformed MEF cell lines for the subsequent analyses. Studies with mitochondrial Txnrd (Txnrd2) revealed that *Txnrd2*^{-/-} cells rapidly die in response to GSH depletion by BSO, a highly specific and irreversible inhibitor of the rate limiting enzyme γ -glutamylcysteine synthetase (γ -GCS) in GSH biosynthesis (15). We therefore treated *Txnrd1*^{-/-} and *Txnrd1*^{fl/fl} cells with increasing concentrations of BSO. Like *Txnrd2*^{-/-} cells, *Txnrd1*^{-/-} cells readily died on treatment with 10 μ mol/L BSO ($3.06 \pm 1.12\%$ viability), whereas the viability of *Txnrd1*^{fl/fl} cells was not affected even at 3-fold higher concentrations of BSO ($100.48 \pm 5.55\%$ viability at 30 μ mol/L BSO; Fig. 4A). We thus conclude that GSH is essential for proliferation and survival of *Txnrd1*^{-/-} cells.

We hypothesized that upregulation or increased activity of GSH-metabolizing enzymes may compensate for the loss of Txnrd1 and thus determined the expression and activity of various key components of the GSH-dependent system in *Txnrd1*^{-/-} cells. *Txnrd1*^{-/-} cells exhibited a 3-fold (3.17 ± 1.5) increase in the transcript of the catalytic subunit (*Gclc*), an 8-fold (7.88 ± 1.76) increase of the modifier subunit (*Gclm*) of γ -GCS, and a 2.5-fold (2.46 ± 0.23) increase in *GSH reductase* (*Gsr*) transcripts compared with *Txnrd1*^{fl/fl} cells (Fig. 4B).

These results were corroborated by measuring the intracellular GSH concentrations and GR activity in *Txnrd1*^{-/-} cells. Total [GSH + oxidized GSH (GSSG)] and reduced GSH levels were 2.7-fold higher in *Txnrd1*^{-/-} cells than in *Txnrd1*^{fl/fl} cells (209.24 ± 68.26 versus 81.21 ± 19.87 μ mol/L/mg protein for total and 186.81 ± 59.94 versus 74.16 ± 17.45 μ mol/L/mg protein for reduced GSH). Likewise, GSSG was 3-fold increased (11.21 ± 4.47 versus 3.52 ± 2.64 μ mol/L/mg protein) in *Txnrd1*^{-/-} cells compared with *Txnrd1*^{fl/fl} cells (Fig. 4C). However, this apparent increase in total (GSH + GSSG), reduced (GSH), and oxidized (GSSG) did not alter the GSH/GSSG redox couple considerably as the ratio of GSH/GSSG remained virtually constant in knockout and wild-type cells (16.6 versus 21.4). Additionally, *Txnrd1*^{-/-} cells exhibited ~ 2.5 -fold higher GR activity than the *Txnrd1*^{fl/fl} cells (2.05 ± 0.36 versus 0.87 ± 0.27 units/mg protein; Fig. 4D).

Reconstitution of Txnrd1 expression in knockout cells reverts the compensatory upregulation of GSH-metabolizing enzymes

To provide definitive proof that the increases in GSH levels and GR activity are indeed caused by the loss of Txnrd1 and are not due to clonal variations, Strep-FLAG-tagged wild-type mouse Txnrd1 (SF-Txnrd1) was expressed in *Txnrd1*^{-/-} cells from the tetracycline-inducible expression vector pRTS-1 (32). Dox-inducible expression of

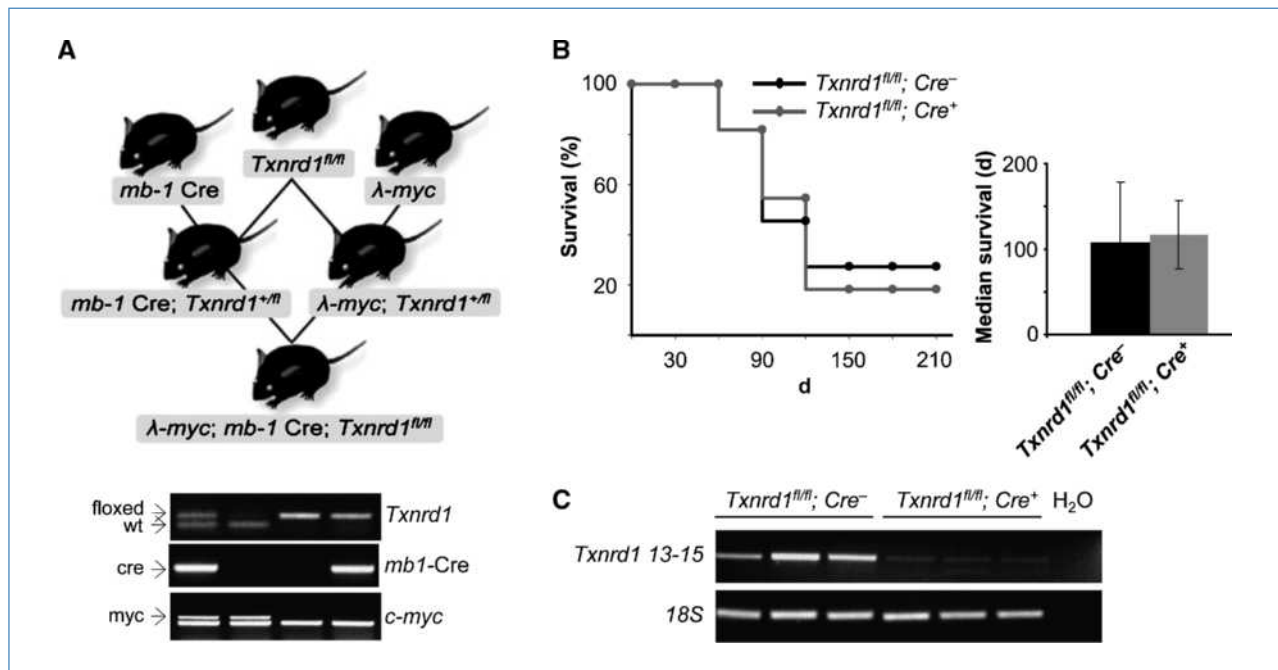


Figure 3. Txnrd1 is dispensable for B-cell lymphomagenesis. **A**, mice breeding scheme to generate Txnrd1-deficient B-cell lymphoma. *Txnrd1*^{fl/fl} mice were crossed with B cell-specific Cre-expressing (*mb-1 Cre*) mice and λ -myc-expressing mice. The resulting mice were then intercrossed to generate mice harboring four transgenic alleles. Genotyping of mice was confirmed by PCR using primer pairs specific for respective transgenes. **B**, Txnrd1 deletion had no effect on the survival of mice succumbing from c-myc-induced lymphomas. The survival time of lymphoma-bearing *Txnrd1*^{fl/fl}; Cre⁺; λ -myc mice (10 of 11) was comparable with that of *Txnrd1*^{fl/fl}; Cre⁻; λ -myc mice (9 of 11) with a median survival of 117 ± 39.4 d (108 ± 69.7 d in control mice; right). **C**, expression of *Txnrd1* was analyzed in tumors by semiquantitative RT-PCR using primer pairs binding in the deleted region. 18S rRNA was used as the product of a housekeeping gene. Faint amplification products were observed in knockout tumors, which most likely derive from contaminating stroma and blood cells.

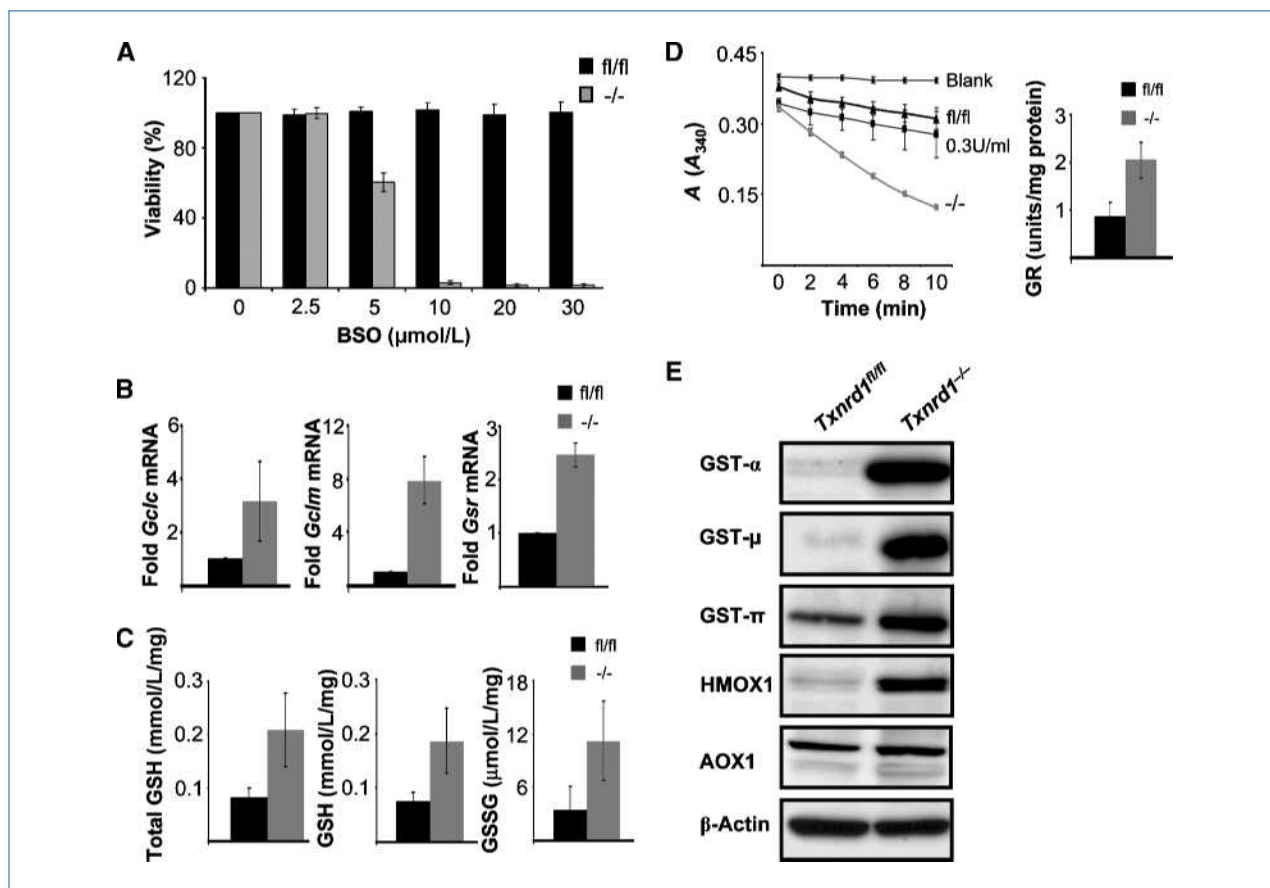


Figure 4. *Txnrd1* null cells are highly sensitive to GSH deprivation due to compensatory upregulation of the GSH system. A, depletion of GSH by BSO for 72 h caused massive cell death of *Txnrd1*^{-/-} cells. Depicted is the percentage of viability representative of three independent experiments with similar results (mean \pm SD). B, quantitative RT-PCR analyses revealed higher expression of key enzymes of the GSH-dependent pathway (*Gclc*, 3.17 \pm 1.5; *Gclm*, 7.88 \pm 1.76; *Gsr*, 2.46 \pm 0.23-fold increased in *Txnrd1*^{-/-} cells compared with *Txnrd1*^{fl/fl} cells). Pooled data from two independent experiments; mean \pm SD (*Gclc*, catalytic; *Gclm*, modifier subunit of γ -GCS). C, total (GSH + GSSG, 209.239 \pm 68.257 versus 81.211 \pm 19.870 μ mol/L/mg protein), reduced (GSH, 186.814 \pm 59.941 versus 74.159 \pm 17.455 μ mol/L/mg protein), and oxidized (GSSG, 11.212 \pm 4.474 versus 3.525 \pm 2.637 μ mol/L/mg protein) GSH were >2.5-fold higher in *Txnrd1*^{-/-} cells compared with *Txnrd1*^{fl/fl} cells; yet, the GSH/GSSG ratio did not change appreciably. Pooled data from four independent experiments; mean \pm SD. D, GR activity was measured by the decrease in absorbance at 340 nm wavelength reflecting the consumption of NADPH (left). *Txnrd1*^{-/-} cells showed ~2.5-fold (2.053 \pm 0.36 units/mg protein) higher GR activity than *Txnrd1*^{fl/fl} cells (0.87 \pm 0.27 units/mg protein). Right, the pooled data from three independent experiments; mean \pm SD. E, immunoblotting against various phase II enzymes revealed that various GSTs and HMOX1, but not AOX1, were upregulated in *Txnrd1*^{-/-} cells compared with parental cells.

SF-Txnrd1 was confirmed by immunoblotting (Fig. 5A). As illustrated in Fig. 5B, *Txnrd1*^{-/-} cells survived treatment with 20 μ mol/L BSO only when Dox (1 μ g/mL) was added to the cell culture medium. This indicates that, in the absence of Txnrd1, survival and proliferation of cells relied on the GSH system.

Next, we asked whether reexpression of Txnrd1 in *Txnrd1*^{-/-} cells may reduce the augmented GSH levels and GR activity (Fig. 5C and D). The total (444.30 \pm 47.86 versus 164.14 \pm 5.05 μ mol/L/mg protein) and reduced (420.66 \pm 41.04 versus 156.34 \pm 1.02 μ mol/L/mg protein) GSH concentrations in untreated *Txnrd1*^{-/-} cells were 2.7-fold higher than in Dox-treated cells. Moreover, Dox treatment caused a 3-fold reduction in GSSG levels (3.90 \pm 3.03 μ mol/L/mg protein) compared with untreated cells (11.82 \pm 3.41 μ mol/L/mg protein; Fig. 5C). As observed before, when GSH and GSSG levels in knockout

and control cells were compared, the GSH/GSSG ratio remained virtually unchanged on reexpression of Txnrd1 (35.5 in untreated cells versus 40.0 in Dox-treated cells). The drop in GSH levels was paralleled by an ~50% reduction in GR activity after Dox addition (2.8 \pm 0.3 versus 1.4 \pm 0.3 units/mg protein; Fig. 5D). The reversal of augmented GSH levels and GR activity on reintroduction of Txnrd1 further lends support to our hypothesis that *Txnrd1*^{-/-} cells upregulate the GSH-dependent pathway as a compensatory mechanism for the missing Txnrd1 function.

Upregulation of phase II enzymes in *Txnrd1*^{-/-} cells

Sengupta and colleagues reported that targeted removal of the gene encoding selenocysteine-specific tRNA (*Trsp*) in liver leads to compensatory upregulation of phase II response genes including GSTs, HMOX1, and AOX1 (41). Given

that Txnrd1 is a selenoprotein, we asked whether Txnrd1 disruption may also affect phase II gene expression in a manner similar to that observed in the selenoprotein-deficient liver. In fact, compensatory upregulation of phase II enzymes (GST and HMOX1) was observed in *Txnrd1*^{-/-} cells, but not of AOX1 (see Fig. 4E).

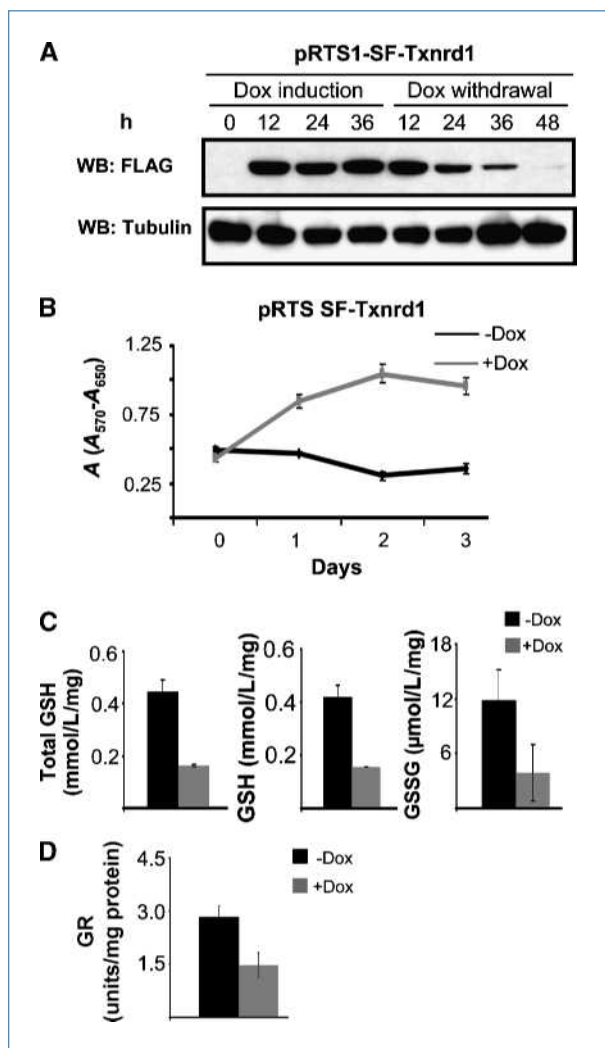


Figure 5. Reconstitution of Txnrd1 reverts the compensatory increase in GSH levels and GR activity. A, Strep-FLAG-tagged Txnrd1 (SF-Txnrd1) was ectopically expressed from a Dox-inducible expression vector. Dox-dependent expression of SF-Txnrd1 was confirmed by immunoblotting using a FLAG-specific antibody. B, proliferation of *Txnrd1*^{-/-} cells after BSO (20 μmol/L) treatment in the presence (1 μg/mL) or absence of Dox. Only in the presence of Dox, *Txnrd1*^{-/-} cells survived the BSO treatment. Data are representative of two independent experiments performed in quadruplicates; mean ± SD. C, Dox treatment caused a 3-fold reduction in total (164.143 ± 5.046 versus 444.308 ± 47.868 μmol/L/mg protein) and reduced (156.343 ± 1.023 versus 420.661 ± 41.042 μmol/L/mg protein) GSH compared with untreated cells. This was accompanied by a 3-fold reduction in GSSG levels (3.900 ± 3.034 versus 11.823 ± 3.413 μmol/L/mg protein); yet, the GSH/GSSG ratio remained unaffected before or after Dox treatment. D, Dox-treated cells revealed an ~50% reduction in GR activity (1.4 ± 0.35 versus 2.8 ± 0.3 units/mg protein; mean ± SD).

Txnrd1^{-/-} tumors are highly susceptible to pharmacologic GSH deprivation

If the growth of *Txnrd1*^{-/-} tumor cells is dependent on the GSH-dependent system also *in vivo*, then pharmacologic intervention of GSH synthesis and/or metabolism might be of substantial therapeutic relevance. To test this, *Txnrd1*^{-/-} tumor-bearing mice (see also Fig. 2D) were treated with 20 mmol/L BSO in the drinking water (Fig. 6A). As shown in Fig. 6B and C, *Txnrd1*^{-/-} tumors were highly susceptible to BSO treatment *in vivo* and only gave rise to very small tumors (0.062 ± 0.05 g) compared with *Txnrd1*^{-/-} tumors (0.48 ± 0.42 g) in untreated mice. The absence of Txnrd1 in these tumors was confirmed by Western blotting (Fig. 6D). Interestingly, no effect of BSO treatment was observed in *Txnrd1*^{fl/fl} tumor-bearing mice (0.40 ± 0.20 g treated versus 0.38 ± 0.32 g untreated tumors). These studies suggest that the growth of Txnrd1-deficient tumors relies on a functional GSH-dependent system and that targeting Txnrd1 alone may not be sufficient to restrain tumor growth.

Discussion

Compelling evidence established that Txnrd1 and in particular Trx1 are upregulated in numerous cancers (21). Given the pro-cancerous function of the Trx system (21–23), both Txnrd1 and Trx1 are suitable candidates for cancer therapy. Here, we addressed two important questions: (a) can Txnrd1 deficiency be compensated by intrinsic mechanisms and (b) is the combined use of drugs simultaneously targeting Trx- and the GSH-dependent systems of potential pharmacologic value to combat cancer?

We show here for the first time that Txnrd1 is dispensable for aggressive tumors and provide evidence for a widespread redundancy between the two major antioxidant systems, the GSH- and Trx-dependent systems, in tumor growth. Although Txnrd1 has been widely regarded as an Achilles' heel for cancer, we failed to recapitulate the findings of previous reports using a well-defined genetic model system (13). Surprisingly, there was no difference in the proliferation, cell cycle distribution, clonogenicity, or tumorigenicity of *c-myc*- and *H-ras*^{v12}-transformed *Txnrd1*^{-/-} cells. Moreover, we could reproduce these results in a *c-myc*-driven B-cell lymphoma mouse model in which we could not find any effect of loss of Txnrd1 on lymphoma incidence and survival of the mice. Furthermore, the increased susceptibility of *Txnrd1*^{-/-} cells toward GSH depletion indicated that the proliferation and survival of *Txnrd1*^{-/-} cells was strictly dependent on the GSH system. The increased susceptibility of tumor cells toward the combined treatment with arsenic (III) oxide that has been reported to inhibit Txnrd1 and BSO (25) can be explained in the light of findings from our present study. A complex cross-talk between the Trx- and GSH-dependent systems has been reported in yeast (42), *Drosophila melanogaster* (43), and *Arabidopsis thaliana* (44); however, the compensatory upregulation of the GSH-dependent system was unprecedented in the context of mammalian tumor growth.

In *Txnrd1*^{-/-} cells, a 2.5- to 3-fold upregulation in total, reduced, and oxidized GSH was observed, which was reversed

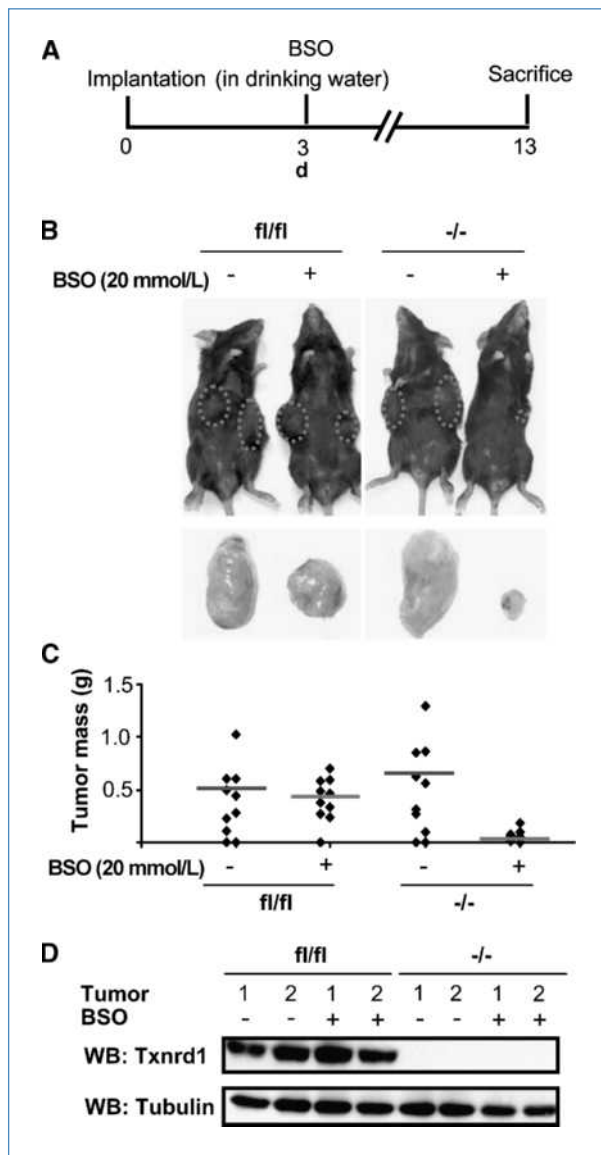


Figure 6. TxnrD1-deficient tumors are highly susceptible to pharmacologic GSH deprivation. **A**, experimental outline for BSO administration in tumor-bearing mice. Transformed cells (1×10^5) were implanted s.c. in C57BL/6 mice and allowed to settle for 3 d. After 3 d, mice were provided with BSO (20 mmol/L) in drinking water for 10 d. Mice were sacrificed on day 13, and the tumor mass was determined. **B** and **C**, *TxnrD1*^{-/-} tumors were highly susceptible to BSO treatment and showed an 8-fold reduction in tumor mass on BSO treatment (0.06 ± 0.05 g) compared with untreated tumors (0.49 ± 0.43 g). *TxnrD1*^{fl/fl} tumors were resistant to BSO treatment (0.40 ± 0.20 ; untreated tumors, 0.38 ± 0.32 g). $n = 10$ (mean \pm SD). **D**, the absence of TxnrD1 was confirmed by immunoblotting using a TxnrD1-specific antibody.

on TxnrD1 reexpression. Remarkably, the GSH/GSSG redox couple and thus the redox potential of GSH/GSSG remained unaltered in knockout cells, which may be due to the corresponding increase in GR activity. By upregulating GR level and activity, *TxnrD1*^{-/-} cells effectively maintain the steady-state redox potential and thereby avoid oxidative

stress. Moreover, upregulation of GSH-synthesizing enzymes and phase II enzymes provides an additional mechanism for the protection of *TxnrD1*^{-/-} cells against oxidative stress.

It should be stressed that cells with a genetic defect in TxnrD1, as reported here, had a better chance to adapt to TxnrD1-independent growth *in vitro* and *in vivo* than wild-type cells in which the enzyme was downregulated by siRNA or targeted by TxnrD1 inhibitors. This may in part explain the discrepancies between our findings and previous reports. Yet, only the genetic system provides the ultimate answer whether compensatory mechanisms exist that may bypass TxnrD1 inhibition and may favor tumor relapse after an initial response to chemotherapy.

Augmented expression of GSH-metabolizing enzymes and phase II enzymes is the probable adaptation mechanism by which *TxnrD1*^{-/-} cells protect themselves from cell death. This induction is presumably mediated through the nuclear factor E2-related factor 2 (Nrf2) and the Kelch-like ECH associated protein 1 (Keap1) system (45). On oxidation of Keap1, Nrf2 is liberated from the cytosolic Keap1/Nrf2 complex and translocates into the nucleus. Nrf2 induces gene expression by binding to the “antioxidant response element” found in many phase II gene promoters including *Gclc*, *Gclm*, and *GR* (*Gsr1*) and GSTs (46). Indeed, knockout of all selenoproteins in liver triggers an Nrf2-dependent upregulation of antioxidant enzymes including HO-1, GCLC, and GSTP1 and combined liver-specific disruption of *Nrf2* and *Trsp* causes hepatocyte dysfunction and impaired survival of compound mutant mice (47). Gene expression profiling of mice lacking liver selenoprotein synthesis revealed independently that many phase II enzymes are induced by selenoprotein loss (41). Hence, one may hypothesize that induction of a fraction of phase II enzymes on *Trsp* removal is mediated in part by TxnrD1 deficiency.

Although cancer cells are susceptible to pharmacologic ROS insults, an upregulation of antioxidant capacity as adaptive response to increased intrinsic oxidative stress might lead to emergence of drug resistance (48). A compensatory upregulation of the GSH-dependent system and phase II enzymes on TxnrD1 deletion and the high susceptibility of TxnrD1-deficient tumors toward pharmacologic inhibition of GSH suggest that simultaneous inhibition of more than one antioxidant systems is particularly efficient in killing tumor cells. Indeed, the redox modifiers like phenethyl isothiocyanate (8) and Motexifen gadolinium (49) have been reported to effectively kill tumor cells by causing the preferential accumulation of ROS, oxidative damage in mitochondria, inactivation of redox-sensitive molecules, and massive cell death.

Simultaneous inhibition of more than one antioxidant system for cancer therapy becomes even more important with the growing evidence that the two key redox systems display widespread redundant functions (35, 50). Recently, we showed that the cystine/cysteine cycle along with TxnrD1 cooperatively rescue GSH deficiency (35). Our data thus rule out a previously alleged indispensable role of TxnrD1 in cancer development. In light of our findings, the use of redox modifiers in cancer treatment should

be exercised with great care due to the extensive cross-talk among the key redox systems.

Disclosure of Potential Conflicts of Interest

No potential conflicts of interest were disclosed.

Acknowledgments

We thank Drs. V. Gladyshev, W. Hammerschmidt, and H. Land for providing the reagents as listed in Materials and Methods; Dr. Dolph Hatfield and Brad Carlson for the generous help for providing the antibodies against the phase II enzymes; Dr. Michael Reth for providing the *mb-1 Cre*

mice; and Drs. Matilde Maiorino and Fulvio Ursini for fruitful discussions. P.K. Mandal thanks Dr. Derrick Rossi for his extended cooperation.

Grant Support

Deutsche Forschungsgemeinschaft (DFG) CO 291/2-1 (M. Conrad), Deutsche Krebshilfe e.V. 10-1979-Bo4 (G.W. Bornkamm), and DFG-Priority Programme SPP1190 (M. Conrad and H. Beck).

The costs of publication of this article were defrayed in part by the payment of page charges. This article must therefore be hereby marked *advertisement* in accordance with 18 U.S.C. Section 1734 solely to indicate this fact.

Received 04/27/2010; revised 08/24/2010; accepted 09/07/2010; published OnlineFirst 11/02/2010.

References

- Sharma SV, Settleman J. Oncogene addiction: setting the stage for molecularly targeted cancer therapy. *Genes Dev* 2007;21:3214–31.
- Weinstein IB, Joe A. Oncogene addiction. *Cancer Res* 2008;68:3077–80; discussion 80.
- Solimini NL, Luo J, Elledge SJ. Non-oncogene addiction and the stress phenotype of cancer cells. *Cell* 2007;130:986–8.
- Luo J, Solimini NL, Elledge SJ. Principles of cancer therapy: oncogene and non-oncogene addiction. *Cell* 2009;136:823–37.
- Schumacker PT. Reactive oxygen species in cancer cells: live by the sword, die by the sword. *Cancer Cell* 2006;10:175–6.
- Kim JH, Chu SC, Gramlich JL, et al. Activation of the PI3K/mTOR pathway by BCR-ABL contributes to increased production of reactive oxygen species. *Blood* 2005;105:1717–23.
- Sattler M, Verma S, Shrikhande G, et al. The BCR/ABL tyrosine kinase induces production of reactive oxygen species in hematopoietic cells. *J Biol Chem* 2000;275:24273–8.
- Trachootham D, Zhou Y, Zhang H, et al. Selective killing of oncogenically transformed cells through a ROS-mediated mechanism by β -phenylethyl isothiocyanate. *Cancer Cell* 2006;10:241–52.
- Szatrowski TP, Nathan CF. Production of large amounts of hydrogen peroxide by human tumor cells. *Cancer Res* 1991;51:794–8.
- Engel RH, Evens AM. Oxidative stress and apoptosis: a new treatment paradigm in cancer. *Front Biosci* 2006;11:300–12.
- Gromer S, Urig S, Becker K. The thioredoxin system—from science to clinic. *Med Res Rev* 2004;24:40–89.
- Nonn L, Williams RR, Erickson RP, Powis G. The absence of mitochondrial thioredoxin 2 causes massive apoptosis, exencephaly, and early embryonic lethality in homozygous mice. *Mol Cell Biol* 2003;23:916–22.
- Jakupoglu C, Przemeczek GK, Schneider M, et al. Cytoplasmic thioredoxin reductase is essential for embryogenesis but dispensable for cardiac development. *Mol Cell Biol* 2005;25:1980–8.
- Matsui M, Oshima M, Oshima H, et al. Early embryonic lethality caused by targeted disruption of the mouse thioredoxin gene. *Dev Biol* 1996;178:179–85.
- Conrad M, Jakupoglu C, Moreno SG, et al. Essential role for mitochondrial thioredoxin reductase in hematopoiesis, heart development, and heart function. *Mol Cell Biol* 2004;24:9414–23.
- Bondareva AA, Capecchi MR, Iverson SV, et al. Effects of thioredoxin reductase-1 deletion on embryogenesis and transcriptome. *Free Radic Biol Med* 2007;43:911–23.
- Soerensen J, Jakupoglu C, Beck H, et al. The role of thioredoxin reductases in brain development. *PLoS ONE* 2008;3:e1813.
- Camier S, Ma E, Leroy C, Pruvost A, Toledano M, Marsolier-Kergoat MC. Visualization of ribonucleotide reductase catalytic oxidation establishes thioredoxins as its major reductants in yeast. *Free Radic Biol Med* 2007;42:1008–16.
- Laurent TC, Moore EC, Reichard P. Enzymatic synthesis of deoxyribonucleotides: IV. Isolation and characterization of thioredoxin, the hydrogen donor from *Escherichia coli* B. *J Biol Chem* 1964;239:3436–44.
- Arner ES, Holmgren A. The thioredoxin system in cancer. *Semin Cancer Biol* 2006;16:420–6.
- Lincoln DT, Ali Emadi EM, Tonissen KF, Clarke FM. The thioredoxin-thioredoxin reductase system: over-expression in human cancer. *Anticancer Res* 2003;23:2425–33.
- Yokomizo A, Ono M, Nanri H, et al. Cellular levels of thioredoxin associated with drug sensitivity to cisplatin, mitomycin C, doxorubicin, and etoposide. *Cancer Res* 1995;55:4293–6.
- Raffel J, Bhattacharyya AK, Gallegos A, et al. Increased expression of thioredoxin-1 in human colorectal cancer is associated with decreased patient survival. *J Lab Clin Med* 2003;142:46–51.
- Lechner S, Muller-Ladner U, Neumann E, et al. Thioredoxin reductase 1 expression in colon cancer: discrepancy between *in vitro* and *in vivo* findings. *Lab Invest* 2003;83:1321–31.
- Lu J, Chew EH, Holmgren A. Targeting thioredoxin reductase is a basis for cancer therapy by arsenic trioxide. *Proc Natl Acad Sci U S A* 2007;104:12288–93.
- Gan L, Yang XL, Liu Q, Xu HB. Inhibitory effects of thioredoxin reductase antisense RNA on the growth of human hepatocellular carcinoma cells. *J Cell Biochem* 2005;96:653–64.
- Yoo MH, Xu XM, Carlson BA, Gladyshev VN, Hatfield DL. Thioredoxin reductase 1 deficiency reverses tumor phenotype and tumorigenicity of lung carcinoma cells. *J Biol Chem* 2006;281:13005–8.
- Yoo MH, Xu XM, Carlson BA, Patterson AD, Gladyshev VN, Hatfield DL. Targeting thioredoxin reductase 1 reduction in cancer cells inhibits self-sufficient growth and DNA replication. *PLoS ONE* 2007;2:e1112.
- Smart DK, Ortiz KL, Mattson D, et al. Thioredoxin reductase as a potential molecular target for anticancer agents that induce oxidative stress. *Cancer Res* 2004;64:6716–24.
- Seiler A, Schneider M, Forster H, et al. Glutathione peroxidase 4 senses and translates oxidative stress into 12/15-lipoxygenase dependent- and AIF-mediated cell death. *Cell Metab* 2008;8:237–48.
- Peitz M, Pfannkuche K, Rajewsky K, Edenhofer F. Ability of the hydrophobic FGF, basic TAT. peptides to promote cellular uptake of recombinant Cre recombinase: a tool for efficient genetic engineering of mammalian genomes. *Proc Natl Acad Sci U S A* 2002;99:4489–94.
- Bornkamm GW, Berens C, Kuklik-Roos C, et al. Stringent doxycycline-dependent control of gene activities using an episomal one-vector system. *Nucleic Acids Res* 2005;33:e137.
- Mosmann T. Rapid colorimetric assay for cellular growth and survival: application to proliferation and cytotoxicity assays. *J Immunol Methods* 1983;65:55–63.
- Fried J, Perez AG, Clarkson BD. Flow cytometric analysis of cell cycle distributions using propidium iodide. Properties of the method and mathematical analysis of the data. *J Cell Biol* 1976;71:172–81.
- Mandal PK, Seiler A, Perisic T, et al. System x(c)- and thioredoxin reductase 1 cooperatively rescue glutathione deficiency. *J Biol Chem* 2010;285:22244–53.
- Mavis RD, Stellwagen E. Purification and subunit structure of glutathione reductase from bakers' yeast. *J Biol Chem* 1968;243:809–14.
- Hobeika E, Thiemann S, Storch B, et al. Testing gene function early

- in the B cell lineage in mb1-Cre mice. *Proc Natl Acad Sci U S A* 2006; 103:13789–94.
38. Kovalchuk AL, Qi CF, Torrey TA, et al. Burkitt lymphoma in the mouse. *J Exp Med* 2000;192:1183–90.
 39. Land H, Parada LF, Weinberg RA. Tumorigenic conversion of primary embryo fibroblasts requires at least two cooperating oncogenes. *Nature* 1983;304:596–602.
 40. Schuhmacher M, Kohlhuber F, Holzel M, et al. The transcriptional program of a human B cell line in response to Myc. *Nucleic Acids Res* 2001;29:397–406.
 41. Sengupta A, Carlson BA, Weaver JA, et al. A functional link between housekeeping selenoproteins and phase II enzymes. *Biochem J* 2008;413:151–61.
 42. Muller EG. A glutathione reductase mutant of yeast accumulates high levels of oxidized glutathione and requires thioredoxin for growth. *Mol Biol Cell* 1996;7:1805–13.
 43. Cheng Z, Arscott LD, Ballou DP, Williams CH, Jr. The relationship of the redox potentials of thioredoxin and thioredoxin reductase from *Drosophila melanogaster* to the enzymatic mechanism: reduced thioredoxin is the reductant of glutathione in *Drosophila*. *Biochemistry* 2007;46:7875–85.
 44. Reichheld JP, Khafif M, Riondet C, Droux M, Bonnard G, Meyer Y. Inactivation of thioredoxin reductases reveals a complex interplay between thioredoxin and glutathione pathways in *Arabidopsis* development. *Plant Cell* 2007;19:1851–65.
 45. Itoh K, Wakabayashi N, Katoh Y, et al. Keap1 represses nuclear activation of antioxidant responsive elements by Nrf2 through binding to the amino-terminal Neh2 domain. *Genes Dev* 1999;13:76–86.
 46. Thimmulappa RK, Mai KH, Srisuma S, Kensler TW, Yamamoto M, Biswal S. Identification of Nrf2-regulated genes induced by the chemopreventive agent sulforaphane by oligonucleotide microarray. *Cancer Res* 2002;62:5196–203.
 47. Suzuki T, Kelly VP, Motohashi H, et al. Deletion of the selenocysteine tRNA gene in macrophages and liver results in compensatory gene induction of cytoprotective enzymes by Nrf2. *J Biol Chem* 2008;283:2021–30.
 48. Trachootham D, Alexandre J, Huang P. Targeting cancer cells by ROS-mediated mechanisms: a radical therapeutic approach? *Nat Rev Drug Discov* 2009;8:579–91.
 49. Hashemy SI, Ungerstedt JS, Zahedi Avval F, Holmgren A. Motexafin gadolinium, a tumor-selective drug targeting thioredoxin reductase and ribonucleotide reductase. *J Biol Chem* 2006;281:10691–7.
 50. Tan SX, Greetham D, Raeth S, Grant CM, Dawes IW, Perrone GG. The thioredoxin-thioredoxin reductase system can function *in vivo* as an alternative system to reduce oxidized glutathione in *Saccharomyces cerevisiae*. *J Biol Chem* 2010;285:6118–26.